Histochemistry and Cell Biology (2020) 154:355–367
https://doi.org/10.1007/s00418-020-01897-3

ORIGINAL PAPER

Unloading during skeletal muscle regeneration retards iNOS-expressing macrophage recruitment and perturbs satellite cell accumulation

Masato Kawashima[1] · Motoi Miyakawa[1,3] · Megumi Sugiyama[1,4] · Makoto Miyoshi[2] · Takamitsu Arakawa[1]

Accepted: 27 June 2020 / Published online: 3 July 2020

Abstract

After skeletal muscle injury, unloading disturbs the regenerative process of injured myofibers, in a manner highly attributed to impairment of macrophage functions. However, the effect of unloading on the spatiotemporal context of proinflammatory macrophage recruitment and satellite cell accumulation within the damaged area remains unclear. This study focused on macrophages expressing inducible nitric oxide synthase (iNOS) that synthesize nitric oxide, a key regulator of muscle regeneration, and compared the continuous hindlimb unloading (HU) by tail suspension *versus* weight-bearing (WB) after skeletal muscle crush injury in rats. We found that in the WB group, the recruitment of iNOS$^+$ proinflammatory macrophages into the injured site gradually increased until their peak number at 48 h post-injury. In the HU group, the accumulation of iNOS$^+$ macrophages until 48 h after injury was significantly less than that in the WB group and continued to increase at 72 h. In accordance with attenuated and/or delayed iNOS$^+$ macrophage recruitment, whole iNOS expression at 24 and 48 h after injury was weakened by unloading. Additionally, in the HU group, satellite cell content of dystrophin-positive non-injured areas diminished at 48 h after injury, and the numbers of activated satellite cells within the regenerating area at 72 and 96 h post-injury were significantly smaller than those in the WB group. These findings suggest that muscle regeneration under unloading conditions results in attenuated and/or delayed recruitment of iNOS$^+$ macrophages and lower iNOS expression in the early phase after muscle injury, leading to perturbed satellite cell accumulation and muscle regeneration.

Keywords Skeletal muscle regeneration · Unloading · Proinflammatory macrophage · iNOS · Satellite cell

Introduction

Loading is one of the regulatory factors for skeletal muscle adaptations. Gravitational unloading such as spaceflight and/or bedrest causes not only atrophy of the skeletal muscle fibers and shift toward a faster myosin heavy chain profile (Ohira et al. 1992; Caiozzo et al. 1994), but also impaired muscle regeneration (Matsuba et al. 2009; Kohno et al. 2012). Unloading conditions after skeletal muscle injury disturb the regenerative process of injured myofibers highly attributed to the impairment of macrophage functions including delayed recruitment into the damaged site, attenuated phagocytic activity, and suppressed properties for myotube formation (Kohno et al. 2012).

Skeletal muscle regeneration is dependent on progressive steps from activation to differentiation of muscle stem cells, called satellite cells (Yin et al. 2013) and is highly orchestrated by macrophages that adopt a sequential inflammatory status during the regenerative process

Electronic supplementary material The online version of this article (https://doi.org/10.1007/s00418-020-01897-3) contains supplementary material, which is available to authorized users.

✉ Takamitsu Arakawa
arakawa@people.kobe-u.ac.jp

[1] Department of Rehabilitation Sciences, Kobe University Graduate School of Health Sciences, 7-10-2 Tomogaoka, Suma-ku, Kobe, Hyogo 654-0142, Japan

[2] Department of Biophysics, Kobe University Graduate School of Health Sciences, Kobe, Japan

[3] Present Address: Yasu Sports Orthopaedics Clinic, 12-16 Wasaka, Akashi, Hyogo 673-0012, Japan

[4] Present Address: General Tokyo Hospital, 3-15-2 Egota, Nakano-ku, Tokyo 165-8906, Japan

Table 1 Actual values of the number of iNOS-expressing macrophages at different time points after muscle injury shown in Fig. 3

	6 h	12 h	24 h	48 h	72 h	96 h
WB	8.2 ± 1.0^{c}	$21.8 \pm 2.2.^{a,c}$	$37.3 \pm 1.5^{a,c}$	$52.2 \pm 4.5^{a,c}$	8.7 ± 1.2^{c}	UC
HU	2.7 ± 0.9	12.0 ± 1.7^{b}	20.8 ± 3.7^{b}	36.6 ± 1.0^{b}	51.4 ± 2.8^{b}	16.1 ± 2.1^{b}

Data are expressed as the mean ± SD, and statistical significance was assessed with two-way ANOVA followed by Bonferroni's multiple comparison test

ANOVA analysis of variance, *HU* hindlimb unloading, *SD* standard deviation, *UC* uncountable, WB weight-bearing

[a] $p < 0.05$ vs. WB at 6 h

[b] $p < 0.05$ vs. HU at 6 h

[c] $p < 0.05$ vs. HU at the same time points. $n = 3$, per group per time point

of damaged muscles (Juban and Chazaud 2017; Tidball 2017). After muscle injury, a massive number of proinflammatory macrophages rapidly accumulate in damaged myofibers prior to satellite cell activation (Kohno et al. 2012). Proinflammatory macrophages then convert into anti-inflammatory macrophages within regenerating muscle fibers (Arnold et al. 2007; Varga et al. 2013). Numerous studies have established that these distinct types of macrophages each exert a specific function throughout the entire process of muscle regeneration (Arnold et al. 2007; Bencze et al. 2012; Saclier et al. 2013).

Nitric oxide, a potent signaling molecule, is synthesized from L-arginine by nitric oxide synthase (NOS) (Stamler and Meissner 2001), and it regulates proper muscle regeneration through modulating the activation and proliferation of satellite cells (Anderson 2000; Filippin et al. 2011; Buono et al. 2012). In the acute phase after muscle injury, neuronal NOS, which is the primary isoform of NOS in skeletal muscles, almost completely disappears (Rigamonti et al. 2013). Meanwhile, inducible NOS (iNOS) rapidly increases and is mostly expressed in macrophages (Rigamonti et al. 2013), suggesting that iNOS derived from macrophages largely contributes to nitric oxide production during the early phase of muscle regeneration.

A previous study revealed that unloading after skeletal muscle injury retards the infiltration of macrophages into the injured site (Kohno et al. 2012). Proinflammatory macrophages that initially invade the damaged myofibers express iNOS and synthesize nitric oxide (Villalta et al. 2009; Tidball and Villalta 2010). Therefore, here we investigated the effect of unloading on the spatiotemporal context of iNOS-expressing macrophage recruitment and satellite cell accumulation after muscle injury to discuss the relationship between proinflammatory macrophages and satellite cells during muscle regeneration. In the present study, we demonstrate that unloading after skeletal muscle injury attenuated and/or delayed the recruitment of iNOS-expressing macrophages. Additionally, these phenomena preceded the perturbation of satellite cell accumulation, causing poor muscle regeneration.

Materials and methods

Animals

Eighty, 8-week-old male Wistar rats weighing 180–200 g (Japan SLC Inc., Shizuoka, Japan) were used. Rats were allowed free access to food and water throughout the experiments. All animals were housed in a controlled environment at 22 °C ± 2 °C with a 12 h light/dark cycle. This study was approved by the Institutional Animal Care and Use Committee and performed according to the Kobe University Animal Experimentation Regulations (approval number: P180706).

Experimental procedures

Muscle injury was induced by crushing the extensor digitorum longus (EDL) muscle according to previous reports (Takagi et al. 2011; Hatade et al. 2014; Takeuchi et al. 2014; Miyakawa et al. 2020). Specifically, animals were anesthetized by isoflurane inhalation, the anterolateral surface of their left hindlimb was shaved, and a longitudinal incision approximately 20 mm long was made to expose the EDL muscle. The middle part of the muscle belly was crushed for 30 s using forceps to which a 500 g weight was attached. Immediately after injury, the skin was closed with a 4–0 suture. Then, animals were randomly divided into two groups: weight-bearing control (WB) and hindlimb unloading (HU). Animals in the WB group were allowed free cage activity throughout the experimental period. In the HU group, hindlimbs of the rats were unloaded immediately after muscle injury until euthanasia, using a previously described method (Morey et al. 1979) with a slight modification. Briefly, tails were wrapped in hypoallergic orthopedic tape and were suspended using a string just high enough to prevent the hindlimbs from bearing weight on the floor or the sides of the cage. The HU rats could reach food and water freely using their forelimbs

during the regenerative process. At 6, 12, 24, 48 h ($n = 7$, respectively), 72 and 96 h, days 7 and 14 ($n = 3$, respectively) after injury, animals were euthanized, and EDL muscles were harvested. The right EDL muscles of all rats were collected as non-injured control. These samples were immediately frozen in dry-ice-cooled acetone and stored at − 80 °C until analysis. The samples at 6, 12, 24, and 48 h after injury were used for morphological analysis ($n = 3$/group at each time point) and for western blot analysis ($n = 4$/group at each time point). The remaining samples at 72 and 96 h, days 7 and 14 were used for morphological analysis ($n = 3$/group at each time point).

During the regenerative processes of the WB and HU groups, the food intake, water consumption, and body weight of each animal were recorded daily. Basically, in both groups, food intake and water consumption per animal per day were similar, which was approximately 20 g in food intake, and was approximately 20 ml in water consumption. In the HU group, only at the measurement of the next day after HU, some animals took a smaller amount of food (10–15 g). However, except for that day, no animals that showed abnormal food intakes and water consumptions were observed in the HU group. Due to the 14 days of regenerative periods, body weights of animals in both WB and HU groups increased (WB, +59.0 ± 4.6 g; HU, +36.0 ± 5.6 g) with significantly smaller increase of body weight in the HU group, compared to the WB group ($P < 0.05$).

Morphological analysis

Transverse cryosections (10 µm) of frozen EDL muscles were obtained by cutting with a cryostat (CM-3050S, Leica Microsystems, Wetzlar, Germany), then these sections were mounted on glass slides. Some sections were used for hematoxylin and eosin (H&E) staining, and others were used for immunohistochemistry as described below. All H&E-stained sections were viewed on an Olympus BX50 microscope (Olympus, Tokyo, Japan) with objectives (UPlanApo 20×/0.70 NA or UPlanApo 40×/0.85 NA, Olympus). Images were recorded with an EOS Kiss X8i camera (max resolution 6000 × 4000 pixels, Canon Inc., Tokyo, Japan) using EOS utility software (Canon Inc.).

Immunohistochemistry

Cryosections were air-dried for 15 min at room temperature, fixed with 4% paraformaldehyde, washed in phosphate-buffered saline (PBS), blocked and permeabilized with PBS containing 10% normal goat serum and 1% Triton X100 for 1 h at room temperature, and incubated with primary antibodies overnight at 4 °C or for 1 h at room temperature. Primary antibodies included mouse monoclonal anti-CD68 antibody (1:200, MCA341GA, Batch# 0515, Bio-Rad, Hercules, CA, USA), rabbit polyclonal anti-iNOS antibody (1:100, ab3523, lot# GR3230433-8, Abcam, Cambridge, UK), mouse monoclonal anti-Pax7 antibody (1:20, sc-81648, lot# G1916, Santa Cruz Biotechnology, Santa Cruz, CA, USA), rabbit polyclonal anti-MyoD antibody (1:400, 18943-1-AP, lot# 00025860, Proteintech, Chicago, IL, USA), and rabbit polyclonal anti-dystrophin antibody (1:200, sc-15376, lot# F0910, Santa Cruz Biotechnology); these were diluted with PBS containing 5% normal goat serum. After washing the sections three times in PBS, samples were visualized using appropriate species-specific Alexa Fluor 488 and/or 568 fluorescence-conjugated secondary antibodies (1:1000, Thermo Fisher Scientific, Waltham, MA, USA) diluted with PBS containing 5% normal goat serum for 2 h at room temperature. After washing in PBS, sections were mounted in Vectashield mounting medium (Vector Laboratories, Burlington, ON, Canada) containing 4′-6-diamino-2-phenylindole (DAPI) to visualize nuclei. Samples were viewed on a ZEISS Axio Vert. A1 with an objective (LD A-Plan 40×/0.55 NA, ZEISS) and photographed with an AxioCam MRm (max resolution 1388 × 1040 pixels) using AxioVision Rel. 4.8 software (ZEISS).

Quantification of muscle regeneration

Muscle regeneration was quantified by measuring cross-sectional area (CSA) of centrally nucleated regenerating myofibers at days 7 and 14 after injury using the method previously described (Lu et al. 2011). Briefly, at × 20 magnification of objective lens, five sections from each specimen separated by ≥ 50 µm underwent H&E staining, and five non-overlapping areas of each section were digitally captured. The distribution of fiber sizes was analyzed from the CSA of centrally nucleated regenerating myofibers and expressed as a percentage of myofibers. Analyses of CSA in all centrally nucleated myofibers were performed on 891.2 ± 138.4 fibers (day 7) and 529.2 ± 152.3 fibers (day 14) per animal using Image J software (http://rsbweb.nih.gov/ij).

Quantitative analyses of iNOS-expressing macrophages and satellite cells

Cell number quantification of iNOS-expressing macrophages and activated satellite cells was performed as described elsewhere (Singh et al. 2017). Briefly, at × 40 magnification of objective lens, 10 fields were captured and quantified for all animals per group and time point. $CD68^+iNOS^+$ cells ($iNOS^+$ macrophages) and $Pax7^+MyoD^+$ cells (activated satellite cells) were counted and expressed as the number of cells per field. The 10 fields were averaged, and a single value was recorded per animal. $iNOS^+$ macrophages in the WB group at 96 h after injury were uncountable, because the injured area was filled up with embryonic (regenerating)

muscle cells that express iNOS (Kaliman et al. 1999) and the macrophages were observed in close proximity to these cells.

To determine satellite cell content of non-injured areas on the injured cross section, double-immunolabeling for Pax7 and dystrophin was performed. Dystrophin is one of cytoskeletal proteins and loss of dystrophin is a great feature of damaged myofibers (Lovering and De Deyne 2004). Therefore, we defined the area that is filled up with dystrophin-positive myofibers as the non-injured area of damaged muscles, and quantified $Pax7^+$ satellite cells observed among the dystrophin-positive non-injured myofibers as previously described (Le Moal et al. 2018). Briefly, at × 20 magnification of objective lens, 10 fields were captured, and the number of $Pax7^+$ cells was counted. Satellite cell content was determined on an average of > 423 fibers per animal and expressed as the number of $Pax7^+$ cells per 100 fibers. All quantitative analyses were performed using Image J software described above, and positive cells were detected by the visual judgment of one observer.

Western blot analysis

Portions (approximately 25 mg) of frozen injured muscle samples were homogenized in PRO-PREP (iNtRON Biotechnology Inc., Gyeonggi-do, Korea). The homogenates were centrifuged at 15,000×*g* for 30 min at 4 °C, and supernatants were collected. Proteins (45 µg/lane) were separated by 7.5% sodium dodecyl sulfate polyacrylamide gel electrophoresis (SDS-PAGE) and transferred to polyvinylidene difluoride (PVDF) membranes (GE Healthcare, Chalfont St Giles, UK). After blocking for 1 h in Tris-buffered saline with Tween 20 (TBS-T) containing 20 g/L skim milk, the membranes were incubated with rabbit polyclonal anti-iNOS antibody (1:500, ab3523, lot# GR3230433-8, Abcam) overnight at 4 °C. The membranes then were incubated for 1 h at room temperature with horseradish peroxidase (HRP)-conjugated anti-rabbit secondary antibody. Blots were developed using the Clarity Max Western ECL Substrate (Bio-Rad) and recorded with OptimaShot CL-420α (Fujifilm Wako Pure Chemical Co., Osaka, Japan). Quantitative analysis was performed using Image J software described above.

Statistical analyses

Data are expressed as the mean ± standard deviation. All experiments were carried out with at least three different animals. Comparisons were performed using the Student's *t* test or two-way (group × time) analysis of variance followed by Bonferroni post hoc test. *P* values < 0.05 were considered statistically significant. Statistical analyses were performed with IBM SPSS Statistics version 22 (SPSS Japan Inc.).

Results

Unloading during muscle regeneration attenuated and/or delayed iNOS-expressing macrophage recruitment and weakened iNOS protein expression

Earlier regenerative process of crush-injured muscle fibers could be seen in the H&E-stained section of both groups (Fig. 1a–c, g–i). By 24 h after injury, polynuclear cells (possibly neutrophils) and mononuclear cells gradually accumulated in necrotic myofibers of both groups (Fig. 1a–c, g–i). In the WB group, necrotic myofibers were filled with invading cells and contour of necrotic myofibers became undetectable at 24 h after injury (Fig. 1c). However, at the same time point of the HU group, inflammatory cell infiltration was dampened and the shape of necrotic myofibers was still recognized (Fig. 1i).

To investigate whether mononuclear cells within the injured site are iNOS-expressing proinflammatory macrophages, double-immunolabeling for CD68 (macrophages) and iNOS was performed. In Figs. 1, 2, $iNOS^+$ macrophages could be detected as double-positive color (yellow) of CD68 and iNOS surrounding the nucleus (DAPI, blue). In the WB group, several $iNOS^+$ macrophages were observed in damaged areas at 6 h after injury (Fig. 1d), and the infiltration of $iNOS^+$ macrophages gradually became more abundant by 24 h post-injury (Fig. 1e, f). On the contrary, the recruitment of $iNOS^+$ macrophages into the injured site was attenuated in the HU group (Fig. 1j–l). At 48 h after injury, in the WB group, massive numbers of $iNOS^+$ macrophages were observed (Fig. 2c). Then the number of these cells rapidly declined at 72 h post-injury (Fig. 2d), concurrently with the emergence of numerous anti-inflammatory macrophages (see Supplementary Fig. 1) and small regenerating muscle cells with central nuclei (Fig. 2b, arrows). By contrast, in the HU group, infiltration of $iNOS^+$ macrophages continued to increase by 72 h (Fig. 2g, h) and regenerating muscle cells could not be detected at 72 h after injury (Fig. 2f). Quantitative analysis showed that until 48 h after injury, the numbers of $iNOS^+$ macrophages within the damaged areas were fewer in the HU group than those in the WB group, but at 72 h after injury, $iNOS^+$ macrophages were more abundant in the HU group than in the WB group (Fig. 3). In the HU group at 96 h after injury, the numbers of $iNOS^+$ macrophages decreased (Fig. 3) and several anti-inflammatory macrophages were observed (see Supplementary Fig. 1). These results demonstrated that unloading attenuated and/or delayed $iNOS^+$ macrophage recruitment to the injured site.

Because $iNOS^+$ macrophages have been identified as major contributors of iNOS expression in the acute phase

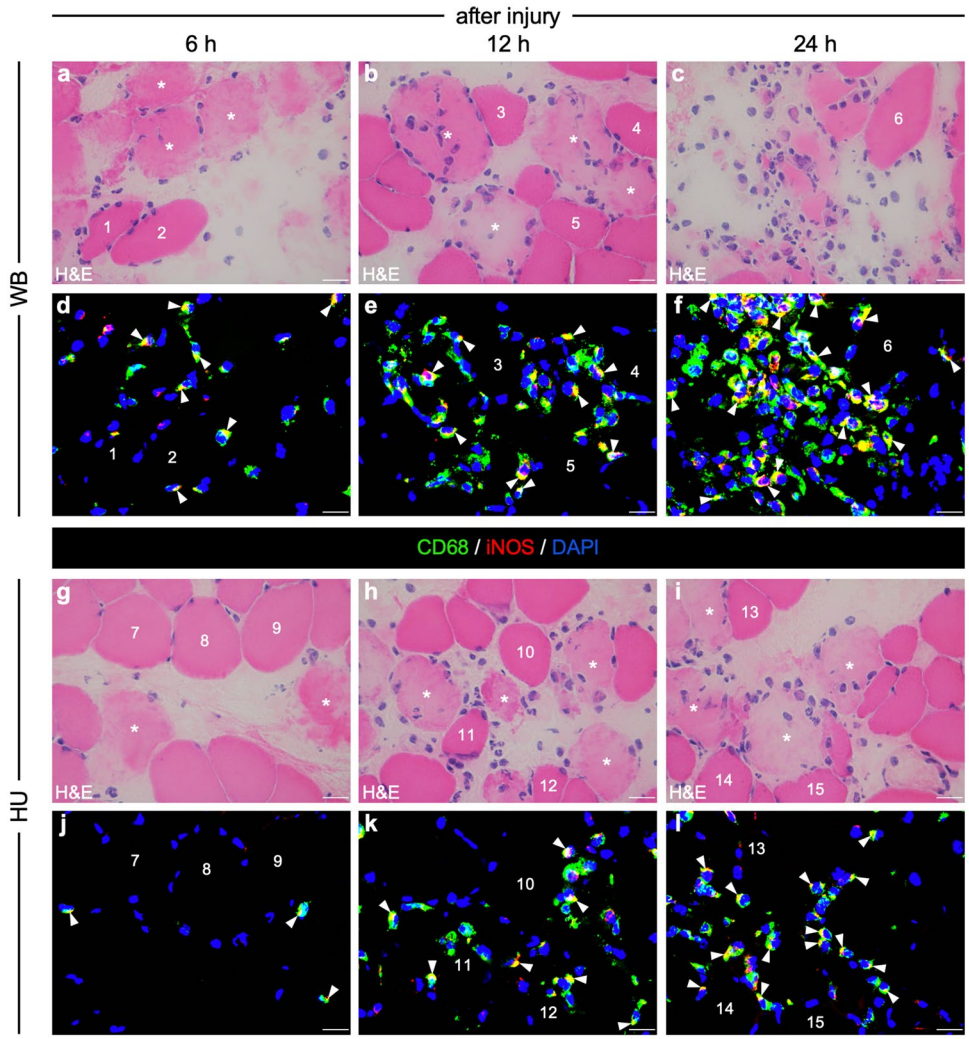

Fig. 1 Morphological characteristics of injured muscles and iNOS-expressing macrophage infiltration at 6, 12, and 24 h after muscle injury. Serial cross sections of injured muscles from the WB (**a**–**f**) and HU (**g**–**l**) groups were analyzed by hematoxylin and eosin staining (**a**–**c**, **g**–**i**), and immunofluorescence (**d**–**f**, **j**–**l**) for CD68 (green, macrophages) and iNOS (red). Nuclei were stained with DAPI (blue; **d**–**f**, **j**–**l**). Arrowheads indicate iNOS-expressing macrophages. These macrophages are identified as double-positive color (yellow) of CD68 and iNOS surrounding the nucleus (blue). The same numbers represent the same myofiber localizations. Scale bars, 20 µm. Abbreviations: DAPI, 4′-6-diamino-2-phenylindole; HU, hindlimb unloading; WB, weight-bearing

after muscle injury (Rigamonti et al. 2013), we next examined whole iNOS expression in injured muscles from the WB and HU groups. iNOS expression was not detected in non-injured muscles (data not shown), and iNOS expression was still scarcely detected in both WB and HU groups until 12 h after injury (Fig. 4a). In the WB group, iNOS expression increased at 24 h and peaked at 48 h after injury (Fig. 4a, b), consistent with the iNOS$^+$ macrophage accumulation shown in Figs. 1, 2, 3. In the HU group, the levels of iNOS expression at 24 and 48 h after injury were lower than those in the WB group (Fig. 4). Surprisingly, iNOS expression level in the HU group at 48 h after injury was still faint (Fig. 4), despite the similar levels of iNOS-expressing macrophage infiltration with the WB group at 24 h post-injury (Fig. 3). Taken together, these data showed that unloading immediately after muscle injury weakened whole iNOS expression in the early phase of muscle regeneration congruently with attenuated and/or delayed iNOS$^+$ macrophage recruitment.

Unloading during muscle regeneration perturbed satellite cell accumulation

To determine whether unloading affects the accumulation of activated satellite cells within the regenerating area, we performed double-immunolabeling for Pax7 (satellite cells) and MyoD. At 48 h after injury, Pax7$^+$MyoD$^+$ cells (activated satellite cells) were hardly detected within the regenerating areas of both WB and HU groups (data not shown). At 72 h after injury, numerous activated satellite cells were noted within the regenerating area in the WB group (Fig. 5d), whereas these cells were almost completely undetected in the HU group (Fig. 5h). The number of activated satellite cells in the HU group at 72 h post-injury (0.1 ± 0.1/field) were smaller than that in the WB group (7.2 ± 0.5/field) (Fig. 5q). At 96 h after injury, the number of activated satellite cells increased in both WB and HU groups (Fig. 5l, p). However, the number of these cells remained smaller in the HU group compared with

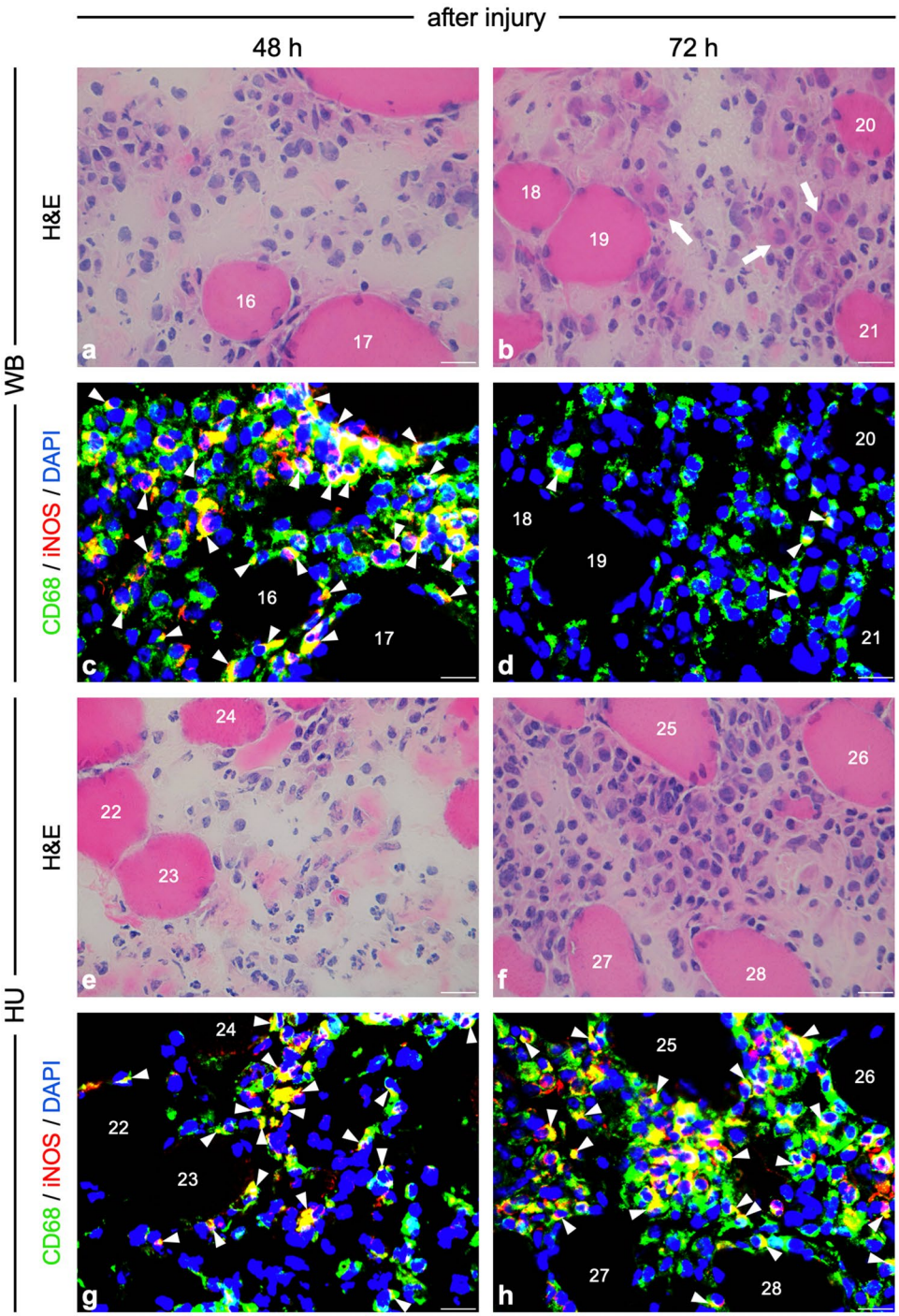

Fig. 2 Morphological characteristics of injured muscles and iNOS-expressing macrophage infiltration at 48 and 72 h after muscle injury. Serial cross sections of injured muscles from the WB (**a**–**d**) and HU (**e**–**h**) groups were analyzed by hematoxylin and eosin staining (**a**, **b**, **e**, **f**), and immunofluorescence (**c**, **d**, **g**, **h**) for CD68 (green, macrophages) and iNOS (red). Nuclei were stained with DAPI (blue; **c**, **d**, **g**, **h**). Arrowheads indicate iNOS-expressing macrophages. These macrophages are identified as double-positive color (yellow) of CD68 and iNOS surrounding the nucleus (blue). The same numbers represent the same myofiber localizations. Scale bars, 20 µm. *DAPI* 4′-6-diamino-2-phenylindole, *HU* hindlimb unloading, *WB* weight-bearing

that of the WB group (WB, 12.3 ± 3.0 vs. HU, 3.77 ± 2.3/field) (Fig. 5q).

Because no satellite cells appeared within the regenerating areas of either WB or HU groups at 48 h after injury, we investigated satellite cell content of non-injured areas on the injured cross section using double-immunolabeling for Pax7 and dystrophin (plasma membrane). $Pax7^+$ satellite cells were observed among dystrophin-positive non-injured myofibers both in the WB and HU groups (Fig. 6a, b). Interestingly, the HU group had fewer satellite cells in the non-injured area compared with those of the WB group (WB, 20.0 ± 0.9 vs. HU, 8.1 ± 1.4/100 fibers) (Fig. 6c). Overall, these results indicated that unloading after muscle injury perturbed the accumulation of satellite cells within the regenerating area.

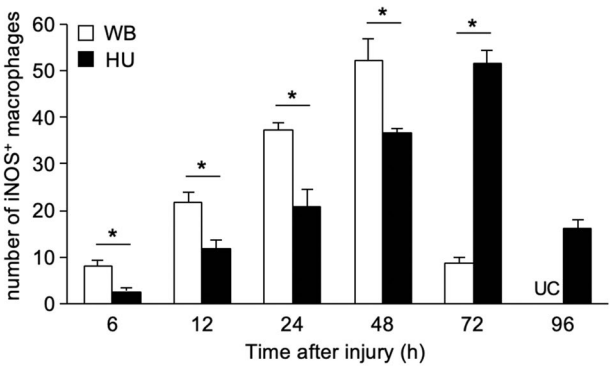

Fig. 3 Chronological changes in the number of iNOS-expressing macrophages after muscle injury. 10 non-overlapping fields per animal were counted ($n=3$, per group per time point). Values are expressed as the mean ± SD, and statistical significance was assessed with two-way ANOVA followed by Bonferroni's multiple comparison test. Statistical differences between groups are only shown. Actual values and all statistical analyses are indicated in Table 1. *$P<0.05$. *ANOVA* analysis of variance, *HU* hindlimb unloading, *SD* standard deviation, *UC* uncountable, *WB* weight-bearing

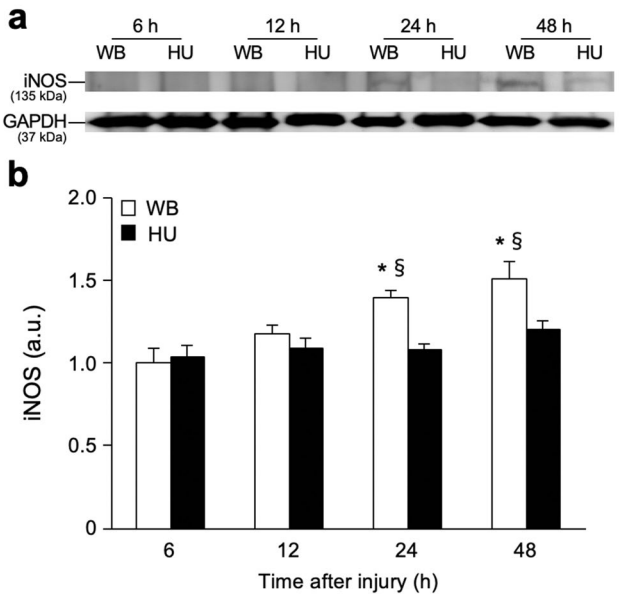

Fig. 4 Time course of the changes in iNOS protein expression after muscle injury. Representative blots (**a**) and quantification of iNOS protein expression in whole muscle lysates of injured muscles from the WB and HU groups at 6, 12, 24, and 48 h after injury (**b**) ($n=4$, per group per time point). The levels of iNOS protein expression were normalized to the GAPDH levels and expressed as the fold changes (a.u.) from the value in the WB group at 6 h after injury. Values are expressed as the mean ± SD, and statistical significance was assessed with two-way ANOVA followed by Bonferroni's multiple comparison test. *$P<0.05$ versus WB at 6 h after injury. §$P<0.05$ versus HU at the same time points. *ANOVA* analysis of variance, *HU* hindlimb unloading, *SD* standard deviation, *WB* weight-bearing

Unloading after muscle injury impaired muscle regeneration

We followed the later regenerative process of injured myofibers in H&E-stained sections in the WB and HU groups until day 14 after injury and evaluated muscle regeneration. At 24 h after injury, numerous inflammatory cells were observed within necrotic fibers in the WB group (Fig. 7b). By 96 h post-injury in the WB group, the accumulation of inflammatory cells was replaced by the appearance of small regenerating myofibers with central nuclei (Fig. 7c). The size of these regenerating myofibers became larger at day 7 (Fig. 7d), and became further mature and the injured areas recovered their normal architecture at day 14 (Fig. 7e). By contrast, the HU group showed the attenuated infiltration of inflammatory cells at 24 h after injury (Fig. 7g). Notably, at 96 h post-injury in the HU group, a large number of mononuclear cells still presented within the necrotic fibers, and regenerating myofibers were scarcely seen (Fig. 7h). By day 14, newly formed myofibers appeared within the regenerating area, and they gradually became larger (Fig. 7i, j). The CSAs of centrally nucleated regenerating myofibers at days 7 and 14 in the HU group were smaller than those in the WB group (day 7: WB, 575.4 ± 100.8 vs. HU, 279.0 ± 53.6 μm^2; day 14: WB, 1803.7 ± 243.8 vs. HU, 728.2 ± 123.3 μm^2) (Fig. 8a, c), and CSA distributions of regenerating myofibers in the HU group showed a general shift toward smaller sizes compared with those of the WB group (Fig. 8b, d). These findings indicated that unloading after skeletal muscle injury jeopardized muscle regeneration.

Discussion

Skeletal muscle regeneration is a tightly coordinated and dynamic process that involves the highly regulated interaction between immune cells and myogenic precursor cells (Saclier et al. 2013; Tidball 2017). Macrophages are the predominant leukocytes observed at each time point of skeletal muscle regeneration following injury, and they exert specific and dynamic functions throughout the entire regenerative process (Chazaud 2016). In the present study, we found that unloading after muscle injury (i) attenuates and/or delays the recruitment of iNOS-expressing proinflammatory macrophages, (ii) delays the emergence of activated satellite cells within the regenerating area, (iii) reduces the satellite cell content of the non-injured area, and (iv) leads to the impairment of muscle regeneration. The present study thus reveals a novel relationship between inflammatory cells and aberrant muscle regeneration under unloading conditions.

The present study shows that attenuated and/or delayed recruitment of iNOS-expressing macrophages (Figs. 1, 2, 3) coincided with the reduced whole iNOS expression (Fig. 4)

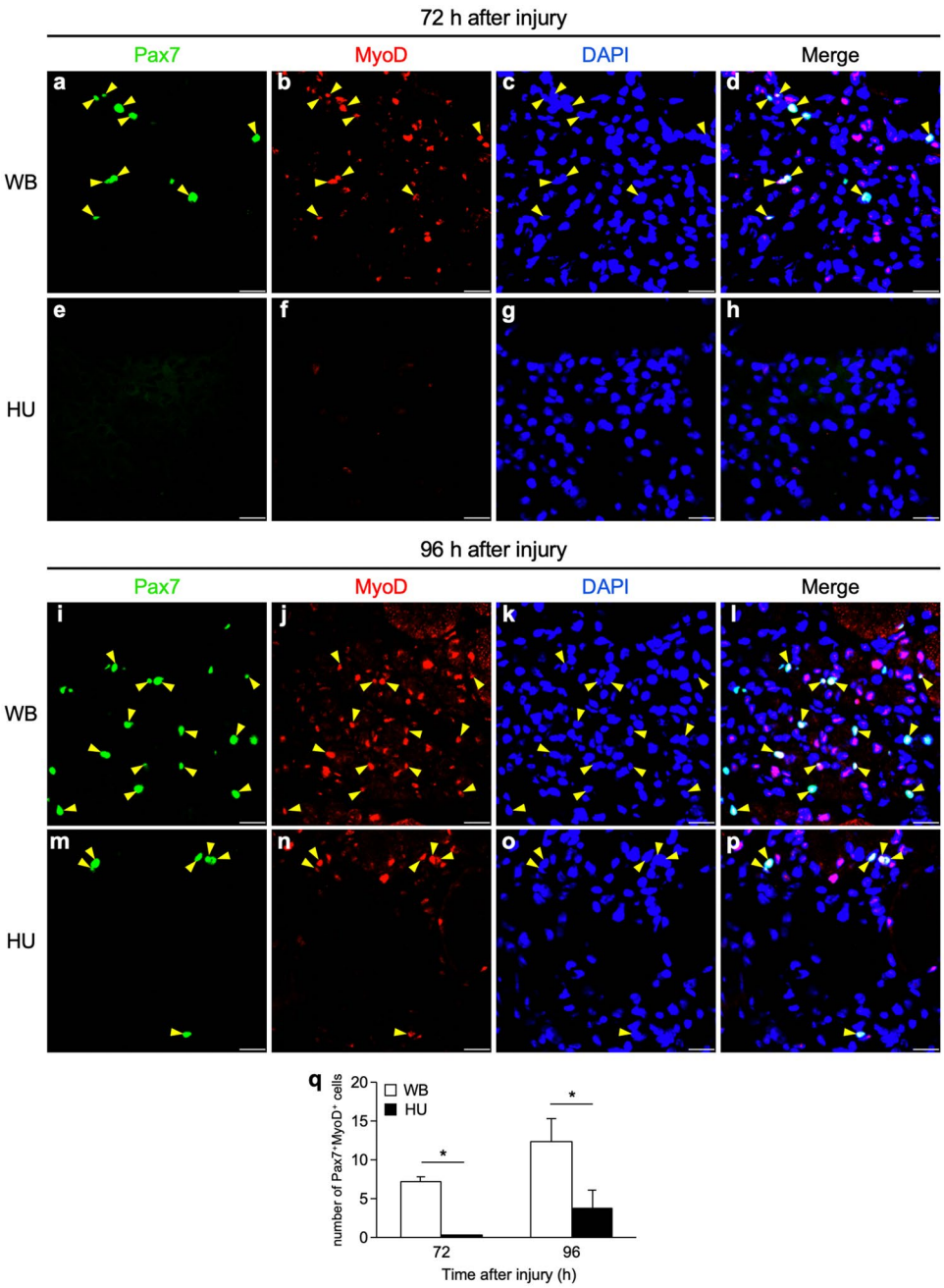

Fig. 5 Activated satellite cell accumulation within the regenerating area at 72 and 96 h after muscle injury. **a**–**p** Representative images of activated satellite cells within the regenerating areas from the WB **a**–**d**, **i**–**l** and HU **e–h**, **m**–**p**) groups after injury. Cross sections from injured muscles were analyzed by immunofluorescence for Pax7 (green, satellite cells) and MyoD (red). Nuclei were stained with DAPI (blue). $Pax7^{+}MyoD^{+}$ activated satellite cells color white in merged images (arrowheads; **d**, **h**, **l**, **p**). Scale bars, 20 µm. **q** Quantification of the number of activated satellite cells at each time point. 10 non-overlapping fields per animal were counted ($n = 3$, per group per time point). Values are expressed as the mean ± SD, and statistical significance was assessed with Student's *t* test. $^{*}P < 0.05$. *DAPI* 4′-6-diamino-2-phenylindole, *HU* hindlimb unloading, *SD* standard deviation, *WB* weight-bearing

in the HU group. During the acute phase of muscle regeneration, iNOS is restrictedly expressed in infiltrating macrophages and modulates early activation and proliferation of satellite cells (Rigamonti et al. 2013). Intriguingly, it was reported that unloading immediately after muscle injury did not alter the mitotic behavior of satellite cells during the early stages of muscle regeneration (Mozdziak et al. 1998). Nevertheless, in the present study, unloading after muscle injury caused the delayed emergence and reduced number of activated satellite cells within the regenerating area (Fig. 5). Moreover, the number of satellite cells localized among the dystrophin-positive non-injured myofibers at 48 h after injury was diminished by unloading (Fig. 6). Therefore, our results suggest that impeded recruitment of iNOS-expressing macrophages is at least partially responsible for perturbed accumulation of satellite cells during muscle regeneration under unloading conditions.

Accumulating evidence suggests that satellite cells not only traverse the entire length of a myofiber but also jump from one fiber to another (e.g., Schultz et al. 1985; Phillips et al. 1990; Siegel et al. 2009) and they migrate in a nitric-oxide-dependent manner (Otto et al. 2011; Collins-Hooper et al. 2012). We found in the present study that unloading after muscle injury retarded the recruitment of

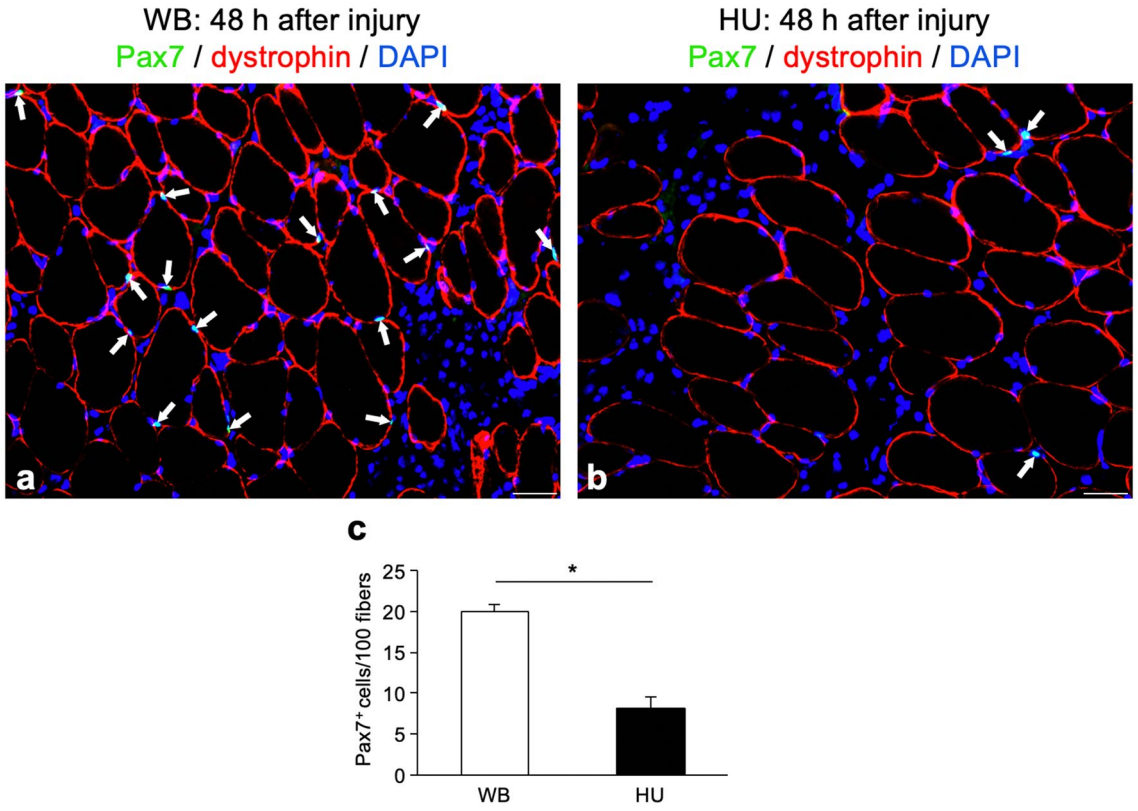

Fig. 6 Satellite cell content of non-injured areas on the injured cross section in both WB and HU groups at 48 h after muscle injury. **a, b** Representative images of satellite cells observed among the dystrophin-positive non-injured myofibers. Immunofluorescence for Pax7 (green) and dystrophin (red) were performed. Nuclei were stained with DAPI (blue). Arrows indicate $Pax7^+$ satellite cells. Scale bars, 20 µm. (**c**) Quantification of the number of satellite cells localized between non-injured myofibers per 100 myofibers ($n=3$, per group). Values are expressed as the mean ± SD, and statistical significance was assessed with Student's t test. $^*P<0.05$. *DAPI* 4′-6-diamino-2-phenylindole, *HU* hindlimb unloading, *SD* standard deviation, *WB* weight-bearing

iNOS-expressing macrophages (Figs. 1, 2, 3), preceding the reduction of satellite cell content of the non-injured area (Fig. 6). Interestingly, iNOS-expressing macrophages were also noted in the interstitial spaces among non-injured myofibers (see Supplementary Fig. 2), indicating the possibility that iNOS-expressing macrophages are associated with satellite cell migration toward the site where regeneration occurs. Thus, we deduce that attenuated and/or delayed recruitment of iNOS-expressing macrophages leads to the perturbed migration of satellite cells into the regenerating area during muscle regeneration under unloading conditions.

Consistent with previous studies (Mozdziak et al. 1998; Kohno et al. 2012), we documented that unloading after muscle injury disturbed muscle regeneration at days 7 and 14 post-injury (Figs. 7, 8). It has been well established that unloading conditions cause atrophy of antigravity muscles, loss of myonuclei, and depressed number of satellite cells (e.g., Goto et al. 2003; Wang et al. 2006). However, EDL muscles might be still under tension due to the abnormal plantar flexion of hindfeet during HU (Riley et al. 1990) and a previous study demonstrated that EDL muscles in rats were not atrophied by 28 days of HU (Zhang et al. 2010). In addition, during post-injury skeletal muscle regeneration, unloaded muscles failed to upregulate atrophy-associated ubiquitin ligases such as MAFbx/Atrogin-1 and MuRF-1, possibly because myofibers were destroyed or immature during the regenerative process (Kohno et al. 2012). Based on these previous findings, there might be negligible effects of lack of tension and muscle atrophy on the jeopardized muscle regeneration in rat EDL muscles shown in the present study.

A limitation of this study is that we did not measure the direct relationship between iNOS-expressing macrophages and satellite cells. In this study, iNOS-expressing macrophage infiltration was followed by the satellite cell accumulation within the regenerative area in both WB and HU groups and unloading perturbed the spatiotemporal context of these cells. However, future studies using in vitro or ex vivo assessments should perform to determine the interaction between iNOS-expressing macrophages and

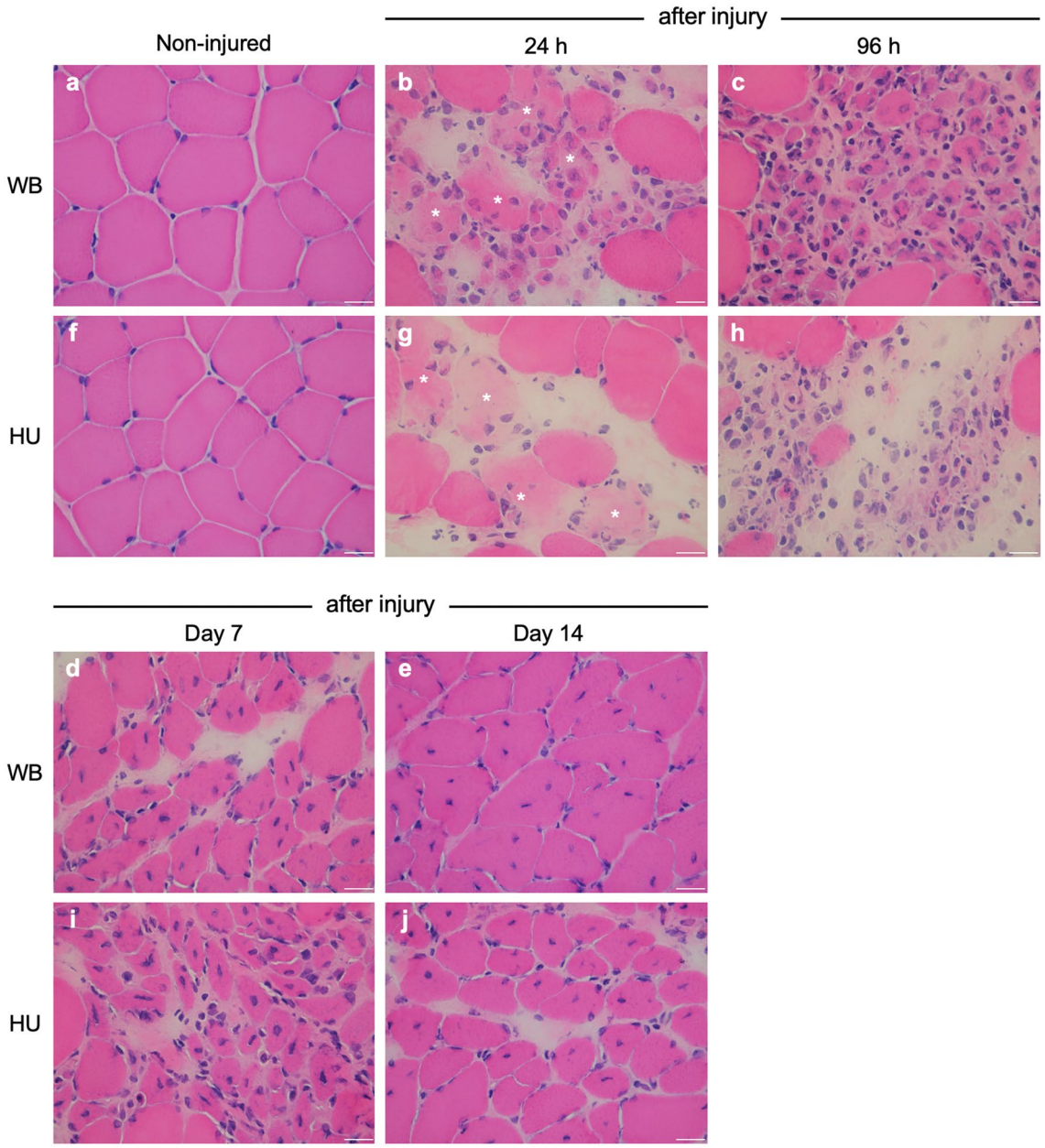

Fig. 7 Histological characterization of muscle regeneration. Muscle cross sections stained with hematoxylin and eosin from the WB and HU groups at non-injured (**a**, **f**), 24 h (**b**, **g**), 96 h (**c**, **h**), days 7 (**d**, **i**) and 14 (**e**, **j**) after muscle injury. Asterisks represent necrotic myofibers. Scale bars, 20 µm. *CSA* cross sectional area, *HU*, hindlimb unloading, *WB* weight-bearing

satellite cells and the effect of unloading on their activities. Another limitation is that we only examined the role of macrophages during muscle regeneration under unloading conditions. Owing to HU, cardiovascular system is altered and stress-relating factors including catecholamine and corticosterone are increased (Globus and Morey-Holton 2016). Macrophage recruitment may also be affected by changes of blood circulation during HU because it has been demonstrated that monocytes/macrophages were recruited from the bone marrow to the blood and then from the blood to injured muscles (Lu et al. 2011) and that once the hindlimbs of the rats were suspended, blood flow to the shaft and marrow in the femur and tibia were already diminished at 10 min after HU (Colleran et al. 2000). Future investigations will address the other potential factors such as vascular aspect and stress response governing the impaired muscle regeneration under unloading conditions.

In conclusion, we demonstrate that unloading after skeletal muscle injury attenuates and/or delays the recruitment of iNOS-expressing proinflammatory macrophages, perturbs

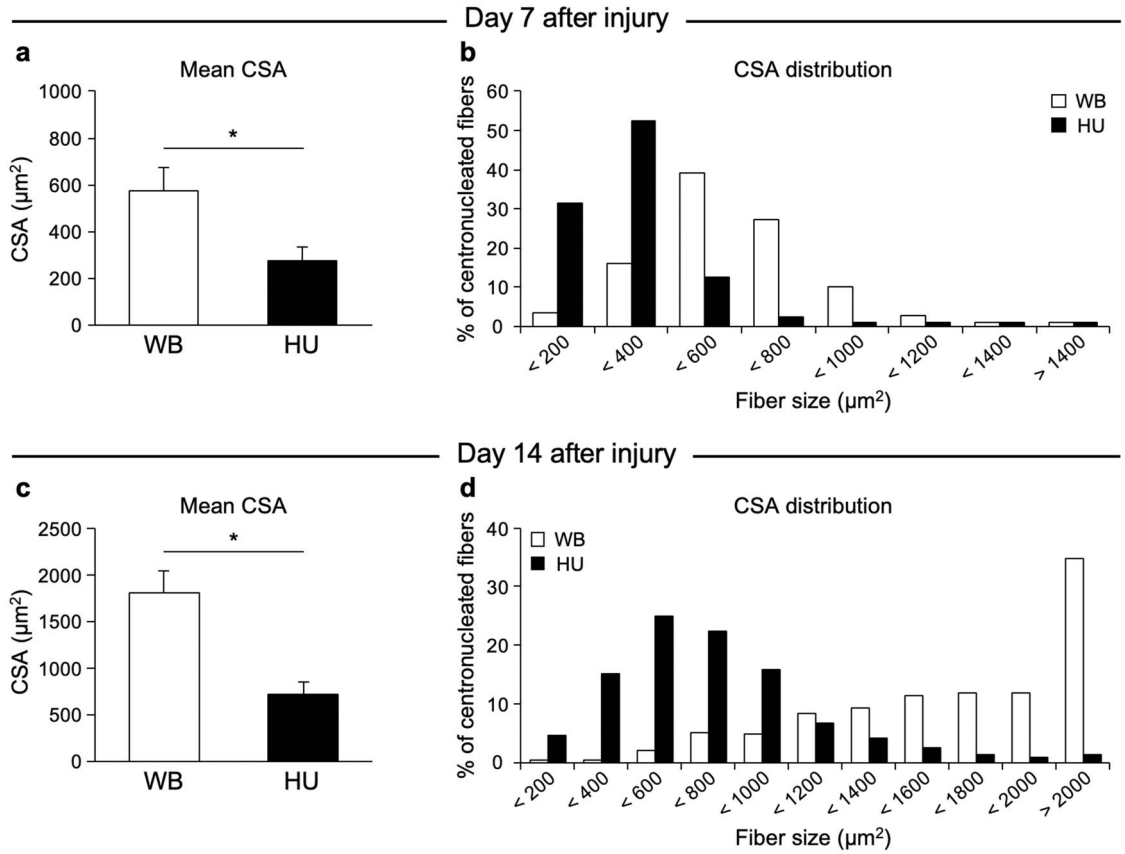

Fig. 8 Evaluation of muscle regeneration at days 7 and 14 after injury. **a**, **c** The mean CSA of centronucleated regenerating myofibers from the WB and HU groups at days 7 (**a**) and 14 (**c**) after injury. **b**, **d** The distribution of regenerating myofiber sizes of the WB and HU groups at days 7 (**b**) and 14 (**d**) after injury. Muscle cross sections stained with hematoxylin and eosin were used to the analyses. Data pooled from > 342 fibers per animal ($n = 3$, per group per time point). Values are expressed as the mean ± SD, and statistical significance was assessed with Student's t test. $^*P < 0.05$. *CSA* cross sectional area, *HU* hindlimb unloading, *SD* standard deviation, *WB* weight-bearing

satellite cell accumulation, and eventually leads to poor muscle regeneration. The present study could enhance our understanding of the relationship between proinflammatory macrophages and satellite cells in the early phase of skeletal muscle regeneration.

Acknowledgments Authors thank the members of our laboratory for their cooperation. We also thank ENAGO (https://www.enago.jp/) for English language editing. This work was supported by Japan Society for the Promotion of Science Grant-in-Aid for scientific research KAKENHI No. 17K01501.

Author contributions Conceptualization: MK and TA; Methodology: MK, MM, MS and TA; Formal analysis and investigation: MK, MM, MS and MM; Writing—original draft preparation: MK; Writing—review and editing: MM, MS and TA; Funding acquisition: TA. All authors read and approved the final manuscript.

Compliance with ethical standards

Conflict of interest The authors declare no conflicts of interest.

References

Anderson JE (2000) A role for nitric oxide in muscle repair: nitric oxide-mediated activation of muscle satellite cells. Mol Biol Cell 11:1859–1874. https://doi.org/10.1091/mbc.11.5.1859

Arnold L, Henry A, Poron F et al (2007) Inflammatory monocytes recruited after skeletal muscle injury switch into antiinflammatory macrophages to support myogenesis. J Exp Med 204:1057–1069. https://doi.org/10.1084/jem.20070075

Bencze M, Negroni E, Vallese D et al (2012) Proinflammatory macrophages enhance the regenerative capacity of human myoblasts by modifying their kinetics of proliferation and differentiation. Mol Ther 20:2168–2179. https://doi.org/10.1038/mt.2012.189

Buono R, Vantaggiato C, Pisa V et al (2012) Nitric oxide sustains long-term skeletal muscle regeneration by regulating fate of satellite cells via signaling pathways requiring Vangl2 and cyclic GMP. Stem Cells 30:197–209. https://doi.org/10.1002/stem.783

Caiozzo VJ, Baker MJ, Herrick RE et al (1994) Effect of spaceflight on skeletal muscle: mechanical properties and myosin isoform content of a slow muscle. J Appl Physiol 76:1764–1773. https://doi.org/10.1152/jappl.1994.76.4.1764

Chazaud B (2016) Inflammation during skeletal muscle regeneration and tissue remodeling: application to exercise-induced muscle

damage management. Immunol Cell Biol 94:140–145. https://doi.org/10.1038/icb.2015.97
Colleran PN, Wilkerson MK, Bloomfield SA et al (2000) Alterations in skeletal perfusion with simulated microgravity: a possible mechanism for bone remodeling. J Appl Physiol 89:1046–1054. https://doi.org/10.1152/jappl.2000.89.3.1046
Collins-Hooper H, Woolley TE, Dyson L et al (2012) Age-related changes in speed and mechanism of adult skeletal muscle stem cell migration. Stem Cells 30:1182–1195. https://doi.org/10.1002/stem.1088
Filippin LI, Cuevas MJ, Lima E et al (2011) Nitric oxide regulates the repair of injured skeletal muscle. Nitric Oxide 24:43–49. https://doi.org/10.1016/j.niox.2010.11.003
Globus RK, Morey-Holton E (2016) Hindlimb unloading: rodent analog for microgravity. J Appl Physiol 120:1196–1206. https://doi.org/10.1152/japplphysiol.00997.2015
Goto K, Okuyama R, Honda M et al (2003) Profiles of connectin (titin) in atrophied soleus muscle induced by unloading of rats. J Appl Physiol 94:897–902. https://doi.org/10.1152/japplphysiol.00408.2002
Hatade T, Takeuchi K, Fujita N et al (2014) Effect of heat stress soon after muscle injury on the expression of MyoD and myogenin during regeneration process. J Musculoskelet Neuronal Interact 14:325–333
Juban G, Chazaud B (2017) Metabolic regulation of macrophages during tissue repair: insights from skeletal muscle regeneration. FEBS Lett 591:3007–3021. https://doi.org/10.1002/1873-3468.12703
Kaliman P, Canicio J, Testar X et al (1999) Insulin-like growth factor-II, phosphatidylinositol 3-kinase, nuclear factor-κB and inducible nitric-oxide synthase define a common myogenic signaling pathway. J Biol Chem 274:17437–17444. https://doi.org/10.1074/jbc.274.25.17437
Kohno S, Yamashita Y, Abe T et al (2012) Unloading stress disturbs muscle regeneration through perturbed recruitment and function of macrophages. J Appl Physiol 112:1773–1782. https://doi.org/10.1152/japplphysiol.00103.2012
Le Moal E, Juban G, Bernard AS et al (2018) Macrophage-derived superoxide production and antioxidant response following skeletal muscle injury. Free Radic Biol Med 120:33–40. https://doi.org/10.1016/j.freeradbiomed.2018.02.024
Lovering RM, De Deyne PG (2004) Contractile function, sarcolemma integrity, and the loss of dystrophin after skeletal muscle eccentric contraction-induced injury. Am J Physiol Cell Physiol 286:230–238. https://doi.org/10.1152/ajpcell.00199.2003
Lu H, Huang D, Saederup N et al (2011) Macrophages recruited via CCR2 produce insulin-like growth factor-1 to repair acute skeletal muscle injury. FASEB J 25:358–369. https://doi.org/10.1096/fj.10-171579
Matsuba Y, Goto K, Morioka S et al (2009) Gravitational unloading inhibits the regenerative potential of atrophied soleus muscle in mice. Acta Physiol 196:329–339. https://doi.org/10.1111/j.1748-1716.2008.01943.x
Miyakawa M, Kawashima M, Haba D et al (2020) Inhibition of the migration of MCP-1 positive cells by icing applied soon after crush injury to rat skeletal muscle. Acta Histochem 122:151511. https://doi.org/10.1016/j.acthis.2020.151511
Morey ER, Sabelman EE, Turner RT, Baylink DJ (1979) A new rat model stimulating some aspects of space flight. Physiologist 22:23–24
Mozdziak PE, Truong Q, Macius A, Schultz E (1998) Hindlimb suspension reduces muscle regeneration. Eur J Appl Physiol 78:136–140. https://doi.org/10.1007/s004210050398
Ohira Y, Jiang B, Roy RR et al (1992) Rat soleus muscle fiber responses to 14 days of spaceflight and hindlimb suspension. J Appl Physiol 73:51–57. https://doi.org/10.1152/jappl.1992.73.2.S51
Otto A, Collins-Hooper H, Patel A et al (2011) Adult skeletal muscle stem cell migration is mediated by a blebbing/amoeboid mechanism. Rejuvenat Res 14:249–260. https://doi.org/10.1089/rej.2010.1151
Phillips GD, Hoffman JR, Knighton DR (1990) Migration of myogenic cells in the rat extensor digitorum longus muscle studied with a split autograft model. Cell Tissue Res 262:81–88. https://doi.org/10.1007/BF00327748
Rigamonti E, Touvier T, Clementi E et al (2013) Requirement of inducible nitric oxide synthase for skeletal muscle regeneration after acute damage. J Immunol 190:1767–1777. https://doi.org/10.4049/jimmunol.1202903
Riley DA, Slocum GR, Bain JL et al (1990) Rat hindlimb unloading: soleus histochemistry, ultrastructure, and electromyography. J Appl Physiol 69:58–66. https://doi.org/10.1152/jappl.1990.69.1.58
Saclier M, Yacoub-Youssef H, Mackey AL et al (2013) Differentially activated macrophages orchestrate myogenic precursor cell fate during human skeletal muscle regeneration. Stem Cells 31:384–396. https://doi.org/10.1002/stem.1288
Schultz E, Jaryszak DL, Valliere CR (1985) Response of satellite cells to focal skeletal muscle injury. Muscle Nerve 8:217–222. https://doi.org/10.1002/mus.880080307
Siegel AL, Atchison K, Fisher KE et al (2009) 3D timelapse analysis of muscle satellite cell motility. Stem Cells 27:2527–2538. https://doi.org/10.1002/stem.178
Singh DP, Lonbani ZB, Woodruff MA et al (2017) Effects of topical icing on inflammation, angiogenesis, revascularization, and myofiber regeneration in skeletal muscle following contusion injury. Front Physiol 8:1–15. https://doi.org/10.3389/fphys.2017.00093
Stamler JS, Meissner G (2001) Physiology of nitric oxide in skeletal muscle. Physiol Rev 81:209–237. https://doi.org/10.1152/physrev.2001.81.1.209
Takagi R, Fujita N, Arakawa T et al (2011) Influence of icing on muscle regeneration after crush injury to skeletal muscles in rats. J Appl Physiol 110:382–388. https://doi.org/10.1152/japplphysiol.01187.2010
Takeuchi K, Hatade T, Wakamiya S et al (2014) Heat stress promotes skeletal muscle regeneration after crush injury in rats. Acta Histochem 116:327–334. https://doi.org/10.1016/j.acthis.2013.08.010
Tidball JG (2017) Regulation of muscle growth and regeneration by the immune system. Nat Rev Immunol 17:165–178. https://doi.org/10.1038/nri.2016.150
Tidball JG, Villalta SA (2010) Regulatory interactions between muscle and the immune system during muscle regeneration. Am J Physiol Regul Integr Comp Physiol 298:1173–1187. https://doi.org/10.1152/ajpregu.00735.2009
Varga T, Mounier R, Gogolak P et al (2013) Tissue LyC6$^-$ macrophages are generated in the absence of circulating LyC6$^-$ monocytes and Nur77 in a model of muscle regeneration. J Immunol 191:5695–5701. https://doi.org/10.4049/jimmunol.1301445
Villalta SA, Nguyen HX, Deng B et al (2009) Shifts in macrophage phenotypes and macrophage competition for arginine metabolism affect the severity of muscle pathology in muscular dystrophy. Hum Mol Genet 18:482–496. https://doi.org/10.1093/hmg/ddn376
Wang XD, Kawano F, Matsuoka Y et al (2006) Mechanical load-dependent regulation of satellite cell and fiber size in rat soleus muscle. Am J Physiol Cell Physiol 290:981–989. https://doi.org/10.1152/ajpcell.00298.2005

Yin H, Price F, Rudnicki MA (2013) Satellite cells and the muscle stem cell niche. Physiol Rev 93:23–67. https://doi.org/10.1152/physrev.00043.2011

Zhang BT, Yeung SS, Liu Y et al (2010) The effects of low frequency electrical stimulation on satellite cell activity in rat skeletal muscle during hindlimb suspension. BMC Cell Biol 11:87. https://doi.org/10.1186/1471-2121-11-87